esteem3

Enabling Science through European Electron Microscopy

Report on ps-resolved STEM-CL experiments

Deliverable D5.1– version 1

Estimated delivery date:	30th June 2021
Actual delivery date:	23rd of June 2021
Lead beneficiary:	CNRS LPS
Person responsible:	Mathieu Kociak
Deliverable type:	☒ R ☐ DEM ☐ DEC ☐ OTHER ☐ ETHICS ☐ ORDP
Dissemination level:	PUBLIC

Grant Agreement No:	823802
Funding Instrument:	Research and Innovation Actions (RIA)
Funded under:	H2020-INFRAIA-2018-1: Integrating Activities for Advanced Communities
Starting date:	01.01.2019
Duration:	48 months

THIS PROJECT HAS RECEIVED FUNDING FROM THE EUROPEAN UNION'S HORIZON 2020 RESEARCH AND INNOVATION PROGRAMME UNDER GRANT AGREEMENT NO **823717**

Revision history log

Version number	Date of release	Author	Summary of changes
V0.1	25/05/2021	Mathieu Kociak	First draft of the deliverable
V1	21/06/2021	Peter van Aken	Approval of the deliverable

Time-Resolved Cathodoluminescence in an Ultrafast Transmission Electron Microscope

We report the first time-resolved cathodoluminescence study performed in a pulsed electron gun TEM. We measured the spatial variation of the lifetime of atomic defects (nitrogen vacancy – NV – center) in nano-diamonds with a sub-nanosecond time resolution and 12 nm spatial resolution. This results are part of a submitted article and are already the focus of some Transnational Access granted request.

Methods

Figure 1-a,c shows a sketch of the experimental set-up ; an Hitachi HF2000 ultrafast transmission electron microscope (UTEM) equipped with an ultra-fast cold-field emission source described in previous articles [1]–[3]. A femtosecond laser generates a 400 fs pulsed electron beam from a sharp tungsten tip. The electrons are then accelerated to 150 keV. The repetition rate is set to 2 MHz. The pulsed electron beam can be focused on the sample within a probe of less than 1 nm, and scanned over the region of interest [2]. A parabolic mirror collects the cathodoluminescence generated by the interaction of the electron beam with the sample and sends it to a multimode optical fiber. The main challenge of cathodoluminescence in a UTEM is the signal to noise ratio as the current of the pulsed electron beam (about 100 of fA on the sample [4]) is much smaller than the one generated with a conventional TEM leading to a drastically decreased CL signal. The large collection angle of the parabolic mirror is therefore essential to collect efficiently the luminescence signal. It is followed by a lens whose numerical aperture is matched to an optical fiber redirecting the CL signal either to an optical spectrometer or to a Single Photon Counting Module (SPCM) connected to a correlator. The numerical matching ensures the lowest possible loss of photon flux, which is essential for these low signal experiments. Using the open-source acquisition software PyMoDAQ [5], we can record either the optical spectrum or the decay trace at each position of the electron beam. In this work, we studied nano-diamonds containing a large number of NV centers [6], [7] with a mean diameter of about 100 nm. The NV center is an atomic defect in the diamond crystal lattice consisting of a substitutional nitrogen atom and a neighboring vacancy, it is a very well-known single photon emitter particularly stable under electron excitation and bright at room temperature[8], [9]. The NV center has two different charge states, the neutral NV^0 and the negatively charged $NV^{(-)}$. Cathodoluminescence spectroscopy is probing almost exclusively the NV^0 state [10]. Figure 1-b displays a typical cathodoluminescence spectrum of nano-diamonds used in this study. It was recorded with a continuous electron beam, at room temperature in a VG HB510 scanning TEM. The zero-phonon line emission is visible at 575 nm as well as the broad sideband associated with phonon-assisted emission from 575 to 800 nm.

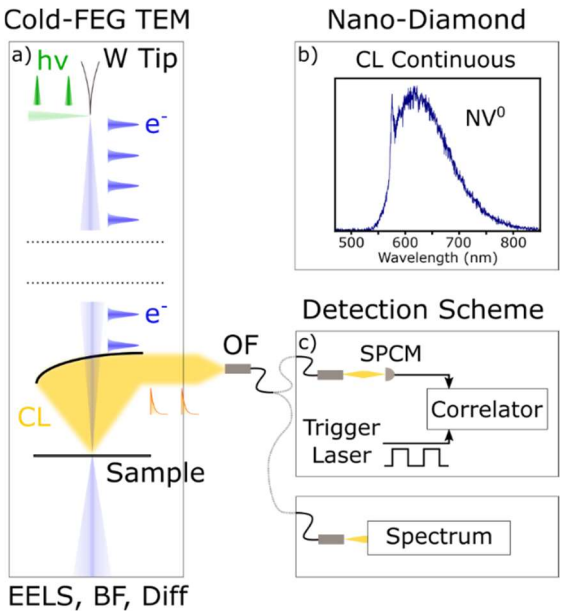

Figure 1: Schematics of the experimental set-up. a) In a modified cold-FEG Hitachi HF2000 microscope, a 2 MHz femto-second laser at 515 nm triggers the emission of femtosecond pulses of electrons from a Tungsten tip. A parabolic mirror collects the cathodoluminescence from the sample. c) Thanks to an optical fiber coupled to the parabolic mirror through a lens (not shown) the light goes either to a spectrometer or to a single photon counting module (SPCM). In the later, a correlator records a histogram of the delays between excitation (trigger) and CL photon detection. Such a histogram forms a decay trace from which the lifetime of the excited state can be extracted. b) Spectrum of a diamond NV^0 center, recorded in a VG510 scanning transmission electron. This spectrum was taken with a continuous beam at room temperature on the same batch of nano-diamonds used for this study. One can see the zero-phonon line at 575 nm followed by the phonon replica from 575 to 800 nm.

Lifetime Measurement

Figure 2 shows the spectrum and decay trace taken for a fixed position of the electron beam on a nano-diamond cluster. In order to maximize the SNR for the acquisition of the CL spectrum (Figure 2-a), no condenser aperture was inserted in the electron column to maximize the electron beam current. This induce a loss in spot size due to geometrical aberrations of condenser lenses. The spectrum acquisition time was 30 s. Nevertheless, we can notice that there is still enough spatial resolution to observe a change in intensity between the two different positions (about 400 nm apart) as noted in the insert of Figure 2-a. The peak at 515 nm visible in the spectrum is mostly due to scattering from the 515 nm laser exciting the Tungsten tip in the electron gun. Direct excitation of the nano-diamonds by the scattered laser light can however be discarded as (i) the number of photons travelling from the tungsten tip to the sample is obviously very low due small apertures size along the electron optics (mainly source extractor and differential aperture), (ii) a significant contribution from such direct optical excitation is not consistent with the observed variations of the signal with the electron beam position and (iii) direct optical excitation of the NV centers would yield a significant contribution from the negatively charged NV^- charge state and was not observed. Figure 2-b displays the decay trace measured at the same position as the blue spectrum of Figure 2-a. To acquire this decay trace, we

record the delay between the excitation (trigger: electronic signal sent from the laser) and the CL photon detection. Due to the correlated acquisition between the excitation and the detection, the SNR improves greatly and we can add an aperture to improve the probe size down to about 5 nm. A long path filter at 550 nm is added in front of the SPCM detector in order to avoid the laser tail visible on the spectrum (Figure 2-a). In these conditions, we detect 40 photons (above the dark noise) per second on the APD. The decay trace displayed in Figure 2-b is taken with an integration time of 200 s.

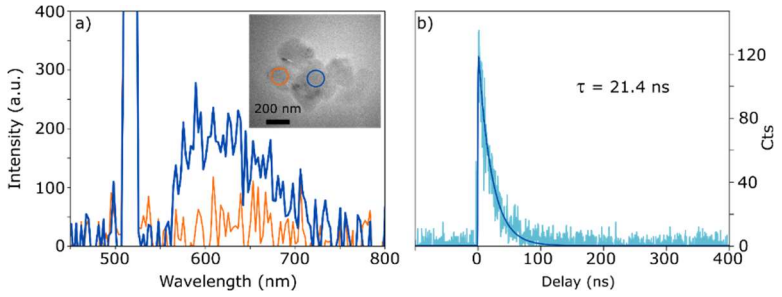

Figure 2 : Spectrum and decay trace measured in the HF2000 based UTEM a) Average spectrum of a nano-diamond cluster (TEM image in Inset). The integration time was 30 s, and no illumination aperture was used to maximize the signal. b) Decay trace recorded for 200 s, the electron probe (5 nm spot using a 70 µm illumination aperture) excited the area highlighted by the blue circle in the inset of a). An exponential fit (thick blue line) gives a lifetime τ of 21.4 ns in the expected range for nano-diamond lifetimes.

In order to extract the lifetime from the decay trace we fit the data with the convolution of an exponential decay and a gaussian. The gaussian function accounts for the time resolution of the experiment. It could also account for a slowly increasing contribution associated to the diffusion of carriers but in the case of nano-diamonds excited by 150 keV electrons we can safely consider the excitation of the defect centers instantaneous compared to the nanosecond lifetime. The instrument response function of the experiment is defined as IRF = $\sqrt{\sum \sigma_i{}^2}$ where σ_i accounts for the different sources of error. In our case the contribution from the electron pulse-width (about 400 fs) is negligible, the time bin is set to 400 ps and the photon detector has a resolution of 350 ps. We therefore expect an IRF of about 530 ps. In the case of Figure 2-b, the fit yields an IRF of 873 ps which is close to what we expect considering the histogram resolution. The lifetime found for the decay trace displayed in Figure 2-b is 21.4 ± 0.5 ns, in the range of expected values for nano-diamonds [11].

These nano-diamonds contain much more than one center. The carrier diffusion length being of the order of 50 nm [12], we expect that the electron beam excites all the centers whatever its position in the nano-diamond. However, the excitation strength of a given center depends on (i) its position inside the diamond and (ii) its position relative to the electron beam. The measured lifetime is therefore an average of the lifetimes of all the centers excited by the electron beam. Nevertheless, lifetime correlation-based measurements performed on similar diamonds have shown a strong disparity of the averaged lifetimes measured between objects [13].

Therefore, we show in Figure 3 the results of spatially-resolved lifetime measurements performed with Time resolved STEM-CL. We scanned the electron beam over the nano-diamonds cluster and recorded a decay trace at each position. Using the same STEM aperture as for the decay trace shown in Figure 2-b (5 nm probe), we scanned a 200 nm region with square pixels of 6 nm width and an integration time of 5s per pixel. Figure 3 – b shows the intensity map extracted from the decay trace map by

summing, for each pixel, all the histogram bin of a 500 ns window (2 MHz repetition rate). We can see quite clearly the intensity variations over the scan depending on the electron beam position. Before fitting each pixel content with the same function as for the average lifetime of Figure 2-b we binned four adjacent pixels to increase the signal to noise ratio. The equivalent integration time is therefore 20 s for each 12 nm width pixel. The lifetime extracted from the fit at each pixel is shown in Figure 3-c. The missing pixels represent pixels lying outside of the diamonds where the signal was too low to perform an accurate fit. Figure 3-d shows two decay traces acquired at different locations on the nano-diamonds and their corresponding fit. The measured lifetime depends strongly on the electron beam position and decreases from 23.4 ns to 15.8 ns when the electron beam is displaced by less than 50 nm. The signal to noise ratio of these spatially-resolved data is worse than in the case of Figure 2. We measured lifetime errors between 0.5 and 1 ns for most pixels and up to 2 ns for the noisiest pixel.

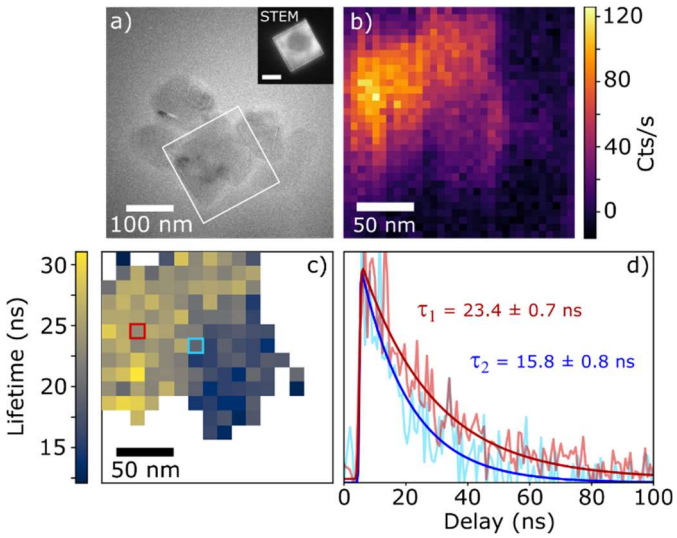

Figure 3 : Lifetime mapping on a Nano-diamond cluster. a) TEM images of the cluster, the white square represents the scanned area. Inset: Scanning probe over the region of interest taken with the TEM CCD camera. scale bar 100 nm b) Intensity map extracted from the decay trace map by summing all the histogram bins of a 500 ns window, pixel size 6.3 nm. c) Lifetime map after binning four adjacent pixels (effective pixel size 12.4 nm). At each pixel a fit of the decay trace has been done and the extracted lifetime reported on the map. Pixels where the signal was too low to extract a lifetime are masked. D) Decay traces and corresponding fit at the locations marked by the blue and red squares in c).

Conclusion and Perspective

To conclude, we have performed the first time-resolved cathodoluminescence experiments in an Ultrafast Transmission Electron Microscope. Due to its high brightness cold-field emission source, this instrument can focus femtosecond electron pulses in a nanometric probe maintaining an optimum brightness. The light emitted from individual emitters is efficiently collected using a high numerical aperture parabolic mirror located close to the sample. This allowed to map the lifetime of NV centers in nano-diamonds with a spatial resolution of about 12 nm and a sub-nanosecond temporal resolution. Such a spatially-resolved lifetime measurements performed using an UTEM are extremely promising to investigate light emission dynamics from complex nanoscale systems [14]. In particular, the possibility of combining information on the emission dynamics together with structural,

morphological, or chemical analysis at the atomic scale will bring invaluable information on the physics of the atomic scale light sources that play an increasing role in opto-electronic devices. This study opens a new application domain for Ultrafast Transmission Electron Microscopes and a wealth of possible experiments combining optical and electron excitation of nanoscale systems.

References:

[1] F. Houdellier, G. M. Caruso, S. Weber, M. Kociak, and A. Arbouet, "Development of a high brightness ultrafast Transmission Electron Microscope based on a laser-driven cold field emission source," *Ultramicroscopy*, vol. 186, pp. 128–138, 2018.

[2] G. M. Caruso, F. Houdellier, S. Weber, M. Kociak, and A. Arbouet, "High brightness ultrafast transmission electron microscope based on a laser-driven cold-field emission source: principle and applications," *Adv. Phys. X*, vol. 4, no. 1, p. 1660214, 2019.

[3] G. M. Caruso, F. Houdellier, P. Abeilhou, and A. Arbouet, "Development of an ultrafast electron source based on a cold-field emission gun for ultrafast coherent TEM," *Appl. Phys. Lett.*, vol. 111, no. 2, 2017.

[4] F. Houdellier, G. M. Caruso, S. Weber, M. J. Hÿtch, C. Gatel, and A. Arbouet, "Optimization of off-axis electron holography performed with femtosecond electron pulses," *Ultramicroscopy*, vol. 202, pp. 26–32, 2019.

[5] S. J. Weber, "PyMoDAQ: An open-source Python-based software for modular data acquisition," *Rev. Sci. Instrum.*, vol. 92, no. 4, p. 45104, 2021.

[6] L.-J. Su *et al.*, "Creation of high density ensembles of nitrogen-vacancy centers in nitrogen-rich type Ib nanodiamonds.," *Nanotechnology*, vol. 24, no. 31, p. 315702, Aug. 2013.

[7] J. Botsoa *et al.*, "Optimal conditions for NV- center formation in type-1b diamond studied using photoluminescence and positron annihilation spectroscopies," *Phys. Rev. B*, vol. 84, no. 12, p. 125209, Sep. 2011.

[8] R. Schirhagl, K. Chang, M. Loretz, and C. L. Degen, "Nitrogen-Vacancy Centers in Diamond: Nanoscale Sensors for Physics and Biology," *Annu. Rev. Phys. Chem.*, vol. 65, no. 1, pp. 83–105, 2014.

[9] A. Mohtashami and a Femius Koenderink, "Suitability of nanodiamond nitrogen–vacancy centers for spontaneous emission control experiments," *New J. Phys.*, vol. 15, no. 4, p. 043017, Apr. 2013.

[10] M. Solà-Garcia, S. Meuret, T. Coenen, and A. Polman, "Electron-induced state conversion in diamond NV centers measured with pump-probe cathodoluminescence spectroscopy," vol. 0, pp. 20–22, Oct. 2019.

[11] H. Lourenço-Martins *et al.*, "Probing Plasmon-NV0 Coupling at the Nanometer Scale with Photons and Fast Electrons," *ACS Photonics*, vol. 5, no. 2, pp. 324–328, 2018.

[12] L. H. G. Tizei and M. Kociak, "Spectrally and spatially resolved cathodoluminescence of nanodiamonds: local variations of the NV(0) emission properties.," *Nanotechnology*, vol. 23, no. 17, p. 175702, 2012.

[13] H. Lourenço-Martins *et al.*, "Probing Plasmon-NV 0 Coupling at the Nanometer Scale with Photons and Fast Electrons," *ACS Photonics*, 2017.

[14] S. Yanagimoto, N. Yamamoto, T. Sannomiya, and K. Akiba, "Purcell effect of nitrogen-vacancy centers in nanodiamond coupled to propagating and localized surface plasmons revealed by

photon-correlation cathodoluminescence," *Phys. Rev. B*, vol. 103, no. 20, p. 205418, 2021.